

## Accepted Manuscript

Design, discovery, modelling, synthesis, and biological evaluation of novel and small, low toxicity *s*-triazine derivatives as HIV-1 non-nucleoside reverse transcriptase inhibitors

Birgit Viira, Anastasia Selyutina, Alfonso T. García-Sosa, Maarit Karonen, Jari Sinkkonen, Andres Merits, Uko Maran

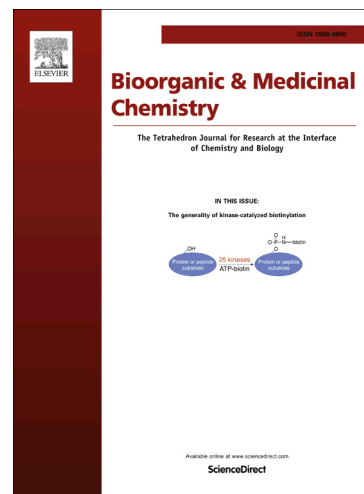
PII: S0968-0896(16)30252-8  
DOI: <http://dx.doi.org/10.1016/j.bmc.2016.04.018>  
Reference: BMC 12933

To appear in: *Bioorganic & Medicinal Chemistry*

Received Date: 28 December 2015  
Revised Date: 10 March 2016  
Accepted Date: 8 April 2016

Please cite this article as: Viira, B., Selyutina, A., García-Sosa, A.T., Karonen, M., Sinkkonen, J., Merits, A., Maran, U., Design, discovery, modelling, synthesis, and biological evaluation of novel and small, low toxicity *s*-triazine derivatives as HIV-1 non-nucleoside reverse transcriptase inhibitors, *Bioorganic & Medicinal Chemistry* (2016), doi: <http://dx.doi.org/10.1016/j.bmc.2016.04.018>

This is a PDF file of an unedited manuscript that has been accepted for publication. As a service to our customers we are providing this early version of the manuscript. The manuscript will undergo copyediting, typesetting, and review of the resulting proof before it is published in its final form. Please note that during the production process errors may be discovered which could affect the content, and all legal disclaimers that apply to the journal pertain.



**Design, discovery, modelling, synthesis, and biological evaluation of novel and small, low toxicity *s*-triazine derivatives as HIV-1 non-nucleoside reverse transcriptase inhibitors.**

Birgit Viira<sup>a</sup>, Anastasia Selyutina<sup>b</sup>, Alfonso T. García-Sosa<sup>a</sup>, Maarit Karonen<sup>c</sup>, Jari Sinkkonen<sup>c</sup>, Andres Merits<sup>b\*</sup>, Uko Maran<sup>a\*</sup>

<sup>a</sup> Institute of Chemistry, University of Tartu, Tartu 50411, Estonia

<sup>b</sup> Institute of Technology, University of Tartu, Tartu 50411, Estonia

<sup>c</sup> Department of Chemistry, University of Turku, FI-20014 Turku, Finland

**Author contributions:**

BV, AS and ATGS have contributed equally.

**Corresponding author:**

\* Phone, +3727375254; fax, +3727375264; e-mail, uko.maran@ut.ee (UM)

\* Phone, +3727375007; e-mail, andres.merits@ut.ee (AM)

**Abstract**

A set of top-ranked compounds from a multi-objective *in silico* screen was experimentally tested for toxicity and the ability to inhibit the activity of HIV-1 reverse transcriptase (RT) in cell-free assay and in cell-based assay using HIV-1 based virus-like particles. Detailed analysis of a commercial sample that indicated specific inhibition of HIV-1 reverse transcription revealed that a minor component that was structurally similar to that of the main compound was responsible for the strongest inhibition. As a result, novel *s*-triazine derivatives were proposed, modelled, discovered, and synthesised, and their antiviral activity and cellular toxicity were tested. Compounds **18a** and **18b** were found to be efficient HIV-1 RT inhibitors, with an IC<sub>50</sub> of 5.6 ± 1.1 μM and 0.16 ± 0.05 μM in a cell-based assay using infectious HIV-1, respectively. Compound **18b** also had no detectable toxicity for different human cell lines. Their binding mode and interactions with the RT suggest that there was strong and adaptable binding in a tight (NNRTI) hydrophobic pocket. In summary, this iterative study produced structural clues and led to a group of non-toxic, novel compounds to inhibit HIV-RT with up to nanomolar potency.

**Keywords:** HIV, non-nucleoside reverse transcriptase inhibitors, synthesis, antiviral activity, molecular docking

**Content**

(Only for reviewing purposes)

|     |  |    |
|-----|--|----|
| 1   | Introduction.....  | 3  |
| 2   | Results and Discussion .....   | 6  |
| 2.1 | Biological activity of in silico screened compounds and their samples .....          | 7  |
| 2.2 | Chemical and biological analysis of active sample .....                              | 8  |
| 2.3 | Proposing novel s-triazine derivatives .....   | 9  |
| 2.4 | Analysis of protein-ligand binding interactions of novel s-triazine derivatives..... | 13 |
| 2.5 | Cytotoxicity and antiviral activity of novel s-triazine derivatives.....             | 17 |
| 3   | Conclusions.....   | 20 |
| 4   | Materials and Methods .....  | 22 |
| 4.1 | In silico screened and selected compounds .....                                      | 22 |
| 4.2 | Computational methods.....   | 22 |
| 4.3 | Chemical synthesis.....  | 23 |
| 4.4 | Materials and instruments. ....  | 27 |
| 4.5 | Cell-culture based assays used for cytotoxicity and anti-HIV-1 activity measurements | 29 |
| 5   | Acknowledgments .....  | 34 |
| 6   | Supplementary data .....   | 35 |
| 7   | References.....  | 36 |

## 1 Introduction

Human immunodeficiency virus type 1 (HIV-1) infection is a serious health threat worldwide: in 2014, a total of 37 million people were living with HIV-1 [1]. The progression of the infection leads to the development of acquired immunodeficiency syndrome (AIDS), which, if untreated, eventually results in patients' deaths, mostly due to opportunistic infections or malignant tumors. To suppress HIV-1 replication, antiretroviral therapy (ART) is used. Currently, ART is a combination of three or more drugs that have different mechanisms of antiviral action. One important group of antiretroviral drugs is Non-Nucleoside Reverse Transcriptase Inhibitors (NNRTIs). Currently, five NNRTIs have been approved by the Food and Drug Administration agency: nevirapine, efavirenz, delavirdine, etravirine, and rilpivirine. They have very different chemical structures but share the same mode of action: their binding to the NNRTI binding pocket of HIV-1 reverse transcriptase (RT) leads to conformational changes in the catalytic subunit of the enzyme and inhibition of its DNA polymerase activity [2]. Because HIV-1 has a high mutation rate during its replication, resistant forms of the virus that are not susceptible to NNRTI treatment arise very quickly. Therefore, new compounds with higher genetic barriers of resistance that are nontoxic for humans are required.

Among the first discovered NNRTI-s were HEPT [3] and diarylpyrimidine (DAPYs) [4] compounds. *In silico* screening has been notably successful in finding new inhibitors for HIV-1 RT. Barreca *et al.* discovered compounds with new molecular scaffolds, including sulfonamides and an oxadiazole that inhibits HIV-1 RT using a structure-based pharmacophore method that includes docking [5]. Jorgensen and co-workers used a pool of inactive compounds from a molecular mechanics-General Born/Surface Area (MM-GB/SA) screen and recovered active compounds by using a substituent scan of core structures placed in the active site [6]. Herschhorn

*et al.* used virtual screening with docking to two protein crystal structures to find thiourea inhibitors against HIV-1 RT [7]. Nichols *et al.* reported HIV-1 RT inhibitors using virtual screening against wild-type (wt) and NNRTI resistant mutant (Y181C) versions of the protein [8]. Among their reported inhibitors, several had structures that included sulphur atoms that were close to conjugated nitrogens or that had an oxazole or cyanouracil group. Physicochemical filters and the rigid docking of conformers led to active compounds against the enzyme [9]. Distinto *et al.* [10] described active sulfonylhydrazone and hydrazone HIV-1 RT inhibitors using a method that was based on shape-based filters, 2D-fingerprints, and 3D-pharmacophore virtual screening that inhibits both DNA polymerase and ribonuclease H (RNase H) activities of HIV-1 RT. Another study showed that docking to X-ray crystal and MD-simulation structures led to two inhibitors [11]. Recent sur-flex docking screening led to the discovery of new dihydroalkoxybenzyloxypyrimidines (DABOs) with modification in the C6 position of the 4(3*H*)-pyrimidinone scaffold [12]. Our own multi-objective *in silico* screening of chemical compound libraries against several protein X-ray crystal structures of wt and NNRTI resistant Y181C HIV-1 RT has resulted in a ranked list of potentially interesting compounds [13]. In that study, protein structures included several conformations of the critical tyrosine 181 residue as well as its substitution for cysteine in addition to the presence or absence of an explicit water molecule in the NNRTI binding pocket. A battery of anti-target proteins was also included in the workflow to profile inhibitor candidates and find compounds that have a moderate-to-low toxicity. The anti-targets included important metabolism proteins, such as the pregnane X receptor, sulfotransferase 1A3, cytochrome P450 2a6, cytochrome P450 2c9, and cytochrome P450 3a4. The resultant compounds had interesting structures, chemistry, and proposed binding modes. The compounds among the top scorers were also profiled and ranked according to the

number of hydrogen bonds they made to backbone atoms of the protein in order to reduce the loss of activity due to a mutation. In addition, compounds were profiled according to their ligand efficiencies [14, 15, 16, 17, 18, 19, 20], which allowed selecting those that were best suited for further development and promising from a physicochemical properties point of view.

The present study experimentally tests the result of the above-described multi-objective *in silico* screening [13] and includes the discovery and synthesis of several new chemical entities from a family of *s*-triazines that were not reported before. The toxicity and antiretroviral activity in the cell-free and cell culture assays of the top-ranked compounds and their derivatives were measured experimentally. The described research shows how the iteration of *in silico* screening and analysis in exploring the NNRTI binding site with chemical compounds can approach systematically closer to the desired result of small, novel, low toxicity NNRT and whole-cell viral HIV inhibitors.

## 2 Results and Discussion

In total, twenty compounds were experimentally tested. First, the 16 commercially available samples (**Figure 1**) were tested for toxicity and antiviral activity. Then, the detected active sample was studied further, and new compounds were proposed, synthesised, and tested for toxicity and antiviral activity. All of the new compounds were supported by computational verification.

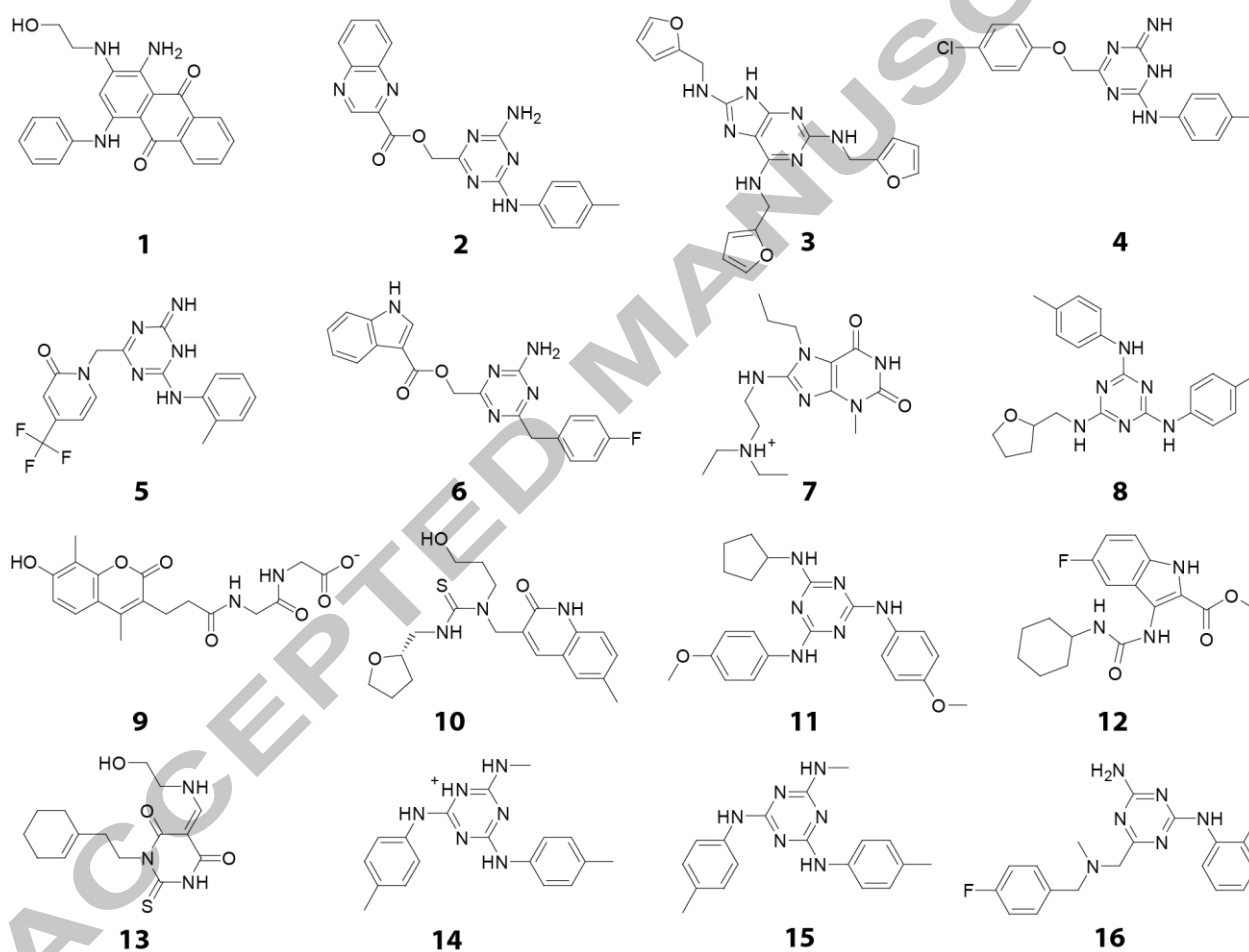


**Figure 1.** Structures of compounds selected from *in silico* screening for toxicity and activity testing.

**Table 1.** Commercial compounds **1-16**, their toxicities and abilities to inhibit HIV-1 activities in different assays.

| Compound          | MW<br>(g/mol) | Toxicity assay,<br>CC <sub>50</sub> , μM | Cell culture assay,<br>IC <sub>50</sub> , μM | Cell free assay,<br>IC <sub>50</sub> , μM |
|-------------------|---------------|--|--|---|
| <b>1</b>          | 373.4         | > 5                                      | > 5  | > 200                                     |
| <b>2</b>          | 387.4         | > 50                                     | > 50   | > 200                                     |
| <b>3</b>          | 405.4         | > 50                                     | > 50   | > 200                                     |
| <b>4</b>          | 341.8         | > 50                                     | > 50   | > 200                                     |
| <b>5</b>          | 376.3         | > 50                                     | > 50   | > 200                                     |
| <b>6</b>          | 378.4         | > 50                                     | > 50   | > 200                                     |
| <b>7</b>          | 323.4         | > 50                                     | > 50   | > 200                                     |
| <b>8</b>          | 390.5         | > 50                                     | 0.33 ± 0.07                                  | 105.7 ± 30                                |
| <b>9</b>          | 375.4         | > 50                                     | > 50   | > 200                                     |
| <b>10</b>         | 389.5         | > 50                                     | > 50   | > 200                                     |
| <b>11</b>         | 406.5         | > 50                                     | > 5  | > 200                                     |
| <b>12</b>         | 347.4         | > 50                                     | > 50   | > 50                                      |
| <b>13</b>         | 323.4         | > 50                                     | > 50   | > 200                                     |
| <b>14</b>         | 319.3         | > 5                                      | > 5  | > 200                                     |
| <b>15</b>         | 319.3         | > 5                                      | > 5  | > 200                                     |
| <b>16</b>         | 320.4         | > 50                                     | > 50   | > 200                                     |
| <b>nevirapine</b> | 266.9         | not toxic                                | 0.42±0.07                                    | 0.92 ± 0.15                               |

### 2.1 Biological activity of *in silico* screened compounds and their samples

We determined the toxicities of 16 commercial samples of compounds at a 50-μM concentration and at a 5-μM concentration for samples that were toxic at 50 μM. Subsequently in cell-culture experiments, the samples were studied only at their corresponding non-toxic or moderate-toxic concentrations (50 μM and/or 5 μM) (**Table 1** and **Table S1**, in supplementary material). The first screen for antiretroviral activities was performed using a virus-like particle (VLP)-based assay because of its increased sensitivity and safety. In addition, the direct effect on the reverse transcription reaction was assessed in a cell-free assay; 200 μM and 50 μM concentrations were used (**Table 1** and **Table S1**, in supplementary material). The highest antiviral activity was observed for **8** (**Figure 1**), and it was the only active sample in both tests (**Table 1**). Subsequent experiments with different concentrations of **8** revealed characteristic sigmoidal inhibition curves (**Figure S1**, in supplementary material). The inhibitory concentration 50 (IC<sub>50</sub>) of **8** in the VLP-based assay was 0.33 ± 0.07 μM, which was only 10 times higher than the IC<sub>50</sub> for the potent known NNRTI nevirapine, which was determined in the same assay. The IC<sub>50</sub> of **8** in a cell-free



assay was  $105.7 \pm 30 \mu\text{M}$  (**Table 2**). A much higher  $\text{IC}_{50}$  in the cell-free reaction, compared to the cell culture assay, has also been shown for NNRTIs elsewhere [21, 22, 23, 24]. The results from these two assays allow to conclude that sample **8** contains an NNRTI HIV-1 inhibitor.

**Table 2.** Anti HIV-1 activities of compound **8** and its derivatives.<sup>a</sup>

|                 | $\text{IC}_{50}$ , $\mu\text{M}$ |                   |                   | $\text{CC}_{50}$ , $\mu\text{M}$ |                |
|-----------------|----------------------------------|-------------------|-------------------|----------------------------------|----------------|
|                 | Cell free assay                  | HIV-1             | VLP (wt)          | TZM-bl (HIV-1)                   | U2OS (VLP)     |
| <b>8</b> (n.p.) | $105.7 \pm 30$                   | ND                | $0.33 \pm 0.07$   | >50                              | >50            |
| <b>8</b>        | NA                               | NA                | $16.0 \pm 3.5$    | >50                              | >50            |
| <b>8</b> (i1)   | NA                               | NA                | $18.2 \pm 5.2$    | >50                              | >50            |
| <b>8</b> (i2)   | NA                               | NA                | $32 \pm 12$       | >50                              | >50            |
| <b>17</b>       | ND                               | ND                | NA                | >50                              | >50            |
| <b>18a</b>      | $116 \pm 12$                     | $5.6 \pm 1.1$     | $2.5 \pm 0.3$     | $57 \pm 22$                      | $42.2 \pm 5.6$ |
| <b>18b</b>      | $55.1 \pm 7.5$                   | $0.16 \pm 0.05$   | $0.067 \pm 0.009$ | >12.5                            | >12.5          |
| <b>19</b>       | ND                               | ND                | NA                | >50                              | >50            |
| nevirapine      | $0.92 \pm 0.15$                  | $0.026 \pm 0.005$ | $0.043 \pm 0.007$ | >100                             | >100           |

<sup>a</sup>  $\text{IC}_{50}$ : the concentration of the compound that is required to inhibit the signal generated by HIV-1 or HIV-1 VLP infection or the activity of purified reverse transcriptase of HIV-1 by 50%;  $\text{CC}_{50}$ : the concentration of the compound that reduces the cell viability (cell index) by 50%; NA – no activity, ND – not determined.

## 2.2 Chemical and biological analysis of active sample

Compound **8** has not been described previously in HIV-1 research in any publication or patent. It contains a diaryltriazine core substituted by three aminoalkyl groups, with two *N-p*-tolyl groups and one *N*-methyltetrahydrofuranlyl group.

The purity of the commercial sample **8** (n.p. – non-purified) was verified by HPLC. Three additional distinctive components (Figure S2), denoted **17**, **18**, and **19**, were detected, which together represented approximately 11% of the mass of the sample. These components were purified to homogeneity with HPLC and collected. Because **17** and **18** failed to be separated well under the used conditions/equipment, a mixture of **17/18** was collected. Because the structure of **8** possessed a chiral centre, its two isomers were also separated with a chiral HPLC column.

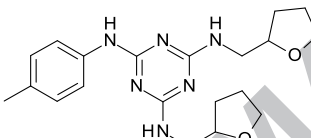
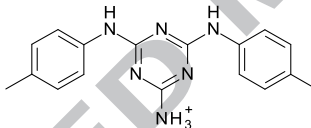
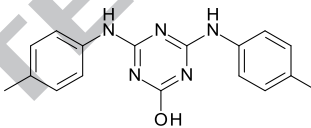
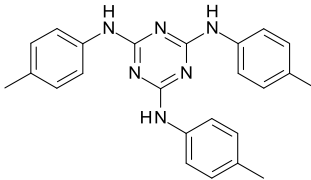
To verify the antiretroviral activity of compound **8**, all of the obtained components of the sample (purified compound **8**(p.), **19**, and mixture **17/18**) and the isomers of **8** were tested for their cytotoxicity and antiviral activity. Testing revealed that purified **8** and its separated isomers as well as **19** did not show prominent antiretroviral activity, whereas the mixture of **17/18** was found to be the most active (**Figure S3**). The mixture of **17/18** also lacked any cytotoxic effect, even at the highest concentration (**Figure S4**). These results allow to conclude that instead of the original belief about compound **8**, components **17** and/or **18** must represent a potent HIV-1 RT inhibitor with a good therapeutic index. This finding also provided the grounds to speculate that the components discovered in the sample could be “side” products from synthesis or intermediates and have structures similar to that of compound **8**. Experimental and analytical testing and verification of the original components **17/18** and **19** were complicated due to the low amount (approximately 0.2 mg) in the commercial sample. Therefore, to identify the structures of **17**, **18**, and **19**, the synthesis methods for compound **8** and its analogs were investigated.

### 2.3 *Proposing novel s-triazine derivatives*

Considering the symmetric nature of the compound **8** core and the molar masses from the mass spectra of the sample components **17/18** and **19** and the synthesis pathways, possible structures (**Table 3: 17, 18a, 18b, and 19**) were proposed. The structures of these new compounds had the same core (1,3,5-triazine) and differed only in the combination of functional groups in substitution positions on the core ring of compound **8**. The molar mass for component **18** was 307.4 g/mol, but considering the possible substitutions, it could match two structures that differ in one substituent (**18a**:  $-\text{NH}_3^+$  or **18b**:  $-\text{OH}$ ). This conclusion led to the use of high-resolution LC-ESI-QTOF-MS to separate the original mixture **17/18** and determine the structure for **18**. The spectrum of **18** exhibited an ion at  $m/z$  308.1530 that corresponded to  $[\text{M}+\text{H}]^+$

( $C_{17}H_{18}N_5O$ , calculated 308.1506, error 7.8 ppm), and the molecular formula for the structure **18** was found to be  $C_{17}H_{17}N_5O$ . The NMR spectrum for the mixture **17/18** was also measured. Comparing the  $^1H$  NMR spectrum with compound **17** showed that the structure of **18** must be rather similar to **17**, but it appeared to be lacking the furan-containing aminoalkyl group, while the tolyl group was easily identified. Based on this arrangement, it was concluded that component **18** must have a structure that contained two amino-tolyl and one hydroxyl group, i.e., compound **18b**.

**Table 3.** Structures for compounds related to **8**, their molecular mass and binding score.

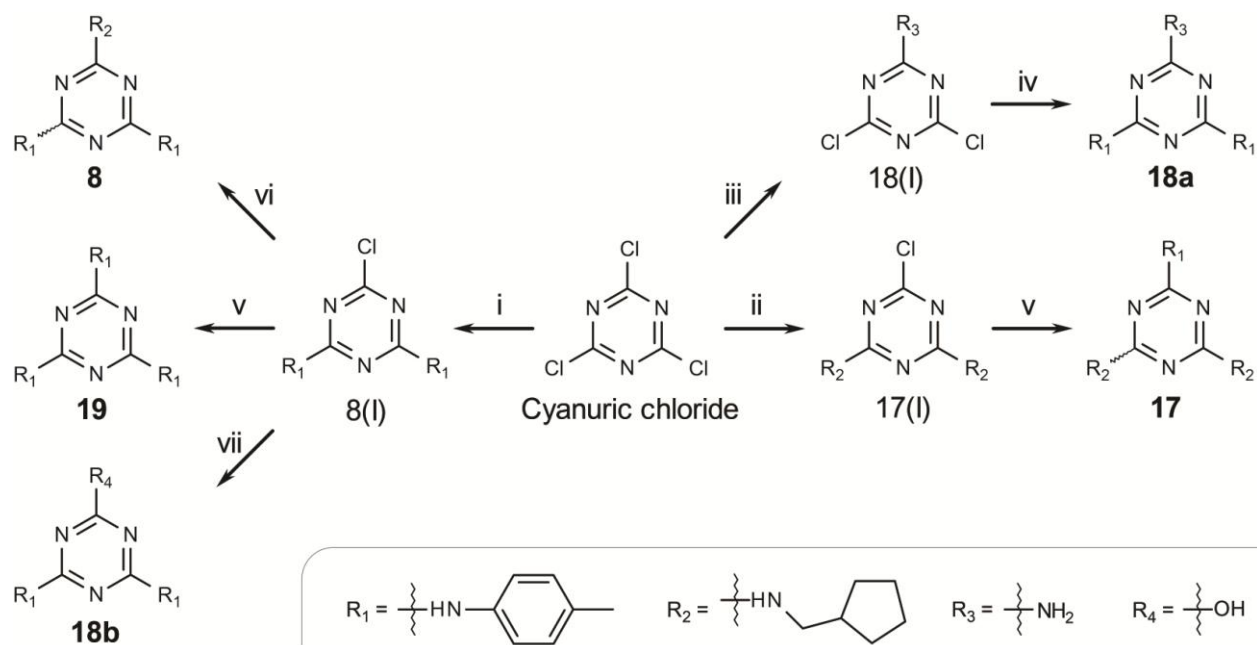
|            | Structure   | MW<br>(g/mol) | Score<br>(kcal/mol) |
|------------|---|---------------|---------------------|
| <b>17</b>  |    | 384.5         | -12.42              |
| <b>18a</b> |  | 307.4         | -14.22              |
| <b>18b</b> |  | 307.4         | -14.36              |
| <b>19</b>  |  | 396.5         | -12.8               |

The proposed structures (**Table 3: 17, 18a, 18b, and 19**) of the sample components were not available from any commercial provider. Consequently, methods for the synthesis of a family of chemical structures with the scaffold (1,3,5-triazines or s-triazines) were adopted from the literature and modified. Even though compound **8** and component **19** did not show prominent

antiretroviral activity (see section 2.2), they were synthesised and tested to verify previous findings with known structure in the case of **19**.

The 1,3,5-triazine derivatives have received substantial attention in the literature because of their potent biological activity as anticancer drugs [25], estrogen receptor modulators [26], antibacterials [27, 28], antimicrobials [28, 29, 30, 31, 32, 33, 34] and also tumor growth inhibition activities [35]. The 1,3,5-triazine derivatives also have several other applications as chiral stationary phases, for the preparation of luminescent complexes and as metal complexes, liquid crystals, calixarenes, dendrimers, and polymers, and as optical brighteners for household washing powders [36]. Considering the above, effort has been devoted for the synthesis of s-triazine derivatives in recent years [36, 37, 38, 39, 40].

After careful consideration of the possible methods for the synthesis of substituted 1,3,5-triazines, the functionalization of the less expensive reagent cyanuric chloride was selected as a promising approach. It has been previously described that the nucleophilic substitution of each chloride is successfully controlled by taking advantage of the decrease in reactivity with the increasing number of substituents [36]. The 2,4,6-substituted 1,3,5-triazines were obtained from cyanuric chloride by sequential substitution of the chloride atom using nitrogen and oxygen centered nucleophiles (**Scheme 1**). Sequential nucleophilic substitution of the C-Cl bond of 1,3,5-triazine by the C-O and C-N bonds has been described elsewhere [36]. In this work, different solvents and substituents were used to achieve the desired products.



**Scheme 1.** General synthetic pathways used for the synthesis of 2,4,6-trisubstituted-1,3,5-triazines. i) cyanuric chloride, *p*-toluene (2 eq), diisopropylamine (2.85 eq), DCM, 0 °C to rt; ii) cyanuric chloride, tetrahydrofuran-4-amine (2 eq), diisopropylamine (2.85 eq), DCM, 0 °C to rt; iii) cyanuric chloride, NH<sub>4</sub>OH (1 eq), DCM, rt; iv) 2,4-dichloro-1,3,5-triazine, tetrahydrofuran-4-amine (2.5 eq), 1,4-dioxane, reflux; v) 2-chloro-1,3,5-triazine, *p*-toluene (1.5 eq), 1,4-dioxane, reflux; vi) 2-chloro-1,3,5-triazine, tetrahydrofuran-4-amine (1.5 eq), 1,4-dioxane, reflux; and vii) 2-chloro-1,3,5-triazine, H<sub>2</sub>O (0.5 eq), dest.H<sub>2</sub>O, TFA, reflux.

This synthesis scheme allowed obtaining large (in gram scale) quantities of **8**, **17**, **18a**, **18b**, and **19** (Table 3). Mono – and di-substituted derivatives of **8** were prepared by the reaction of cyanuric chloride with the corresponding aminoalkyl group in DCM using di-isopropyl amine as a base. Di-substituted derivatives were achievable by performing the reaction at ambient temperature (methods i and ii, **Scheme 1**). To obtain the monosubstituted compound, the reaction had to be carried out at 0°C or below. In case of substitution of the first chlorine with an amino group, the solution was kept at room temperature, and the reaction finished rapidly (method iii, **Scheme 1**). The substitution of the remaining chloride atom(s) usually required considerably more vigorous reaction conditions (such as higher temperatures and longer reaction time) (methods iv-vi, **Scheme 1**).

#### 2.4 Analysis of protein-ligand binding interactions of novel *s*-triazine derivatives.

The docking of compounds **17**, **18a**, **18b** and **19** into the NNRTI binding site of protein structure 2be2 [41], similar to that conducted during virtual screening [13], resulted in a ranking (**18b** > **18a** > **19** > **17**), which is presented in **Table 3**. The triazine chemical motif that is shared between the compounds was indeed present in some of the compounds that were identified in the previous *in silico* screen.

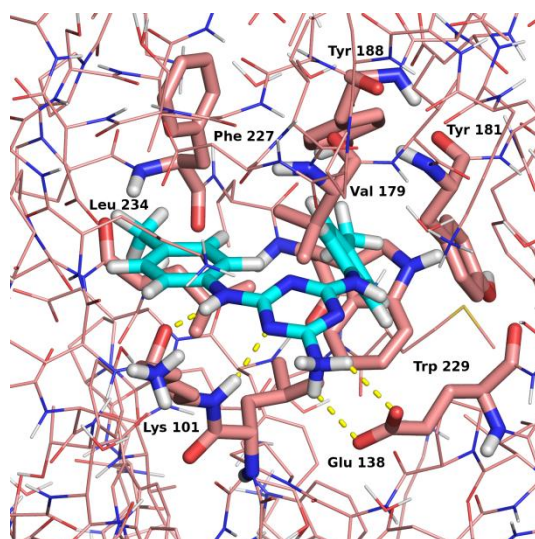


**Figure 2.** Docked binding mode of compound **18a** with the HIV-1 RT crystal structure. Hydrogen atoms are in white, oxygen atoms are in red, and nitrogen atoms are in blue. Ligand carbon atoms are in cyan, and protein carbon atoms are in pink. All of the hydrogen atoms are shown for the ligand, and the polar hydrogens are shown for the protein. Compound **18a** donates a hydrogen bond and accepts a hydrogen bond (yellow dashes) from Lys101, as well as forming an ionic interaction with the sidechain of Glu138. Hydrophobic contacts are provided by the sidechains of Phe 227, Tyr181, Tyr 188, Val 179, and Trp229.

Further detailed computational analysis of the compound **18a** binding mode to the protein (see **Figure 2**) shows that **18a** binds deep into the NNRTI pocket, with its *p*-tolyl groups engaging in  $\pi$ - $\pi$  interactions with residues Tyr 181, Tyr 188, Trp 229, and Phe 227. It also possesses hydrophobic contacts with residues Leu 234 and Val 179, the former interacting with the central ligand heterocycle. It has hydrogen bonds with the backbone C=O and NH groups of

Lys 101 as well as a strong ionic interaction between its charged ammonium group with the charged carboxylic group of Glu 138, at the mouth of the binding site.

Compound **18a** has a low molecular weight of 307.4 g/mol, which enables further modification of the ligand, and it has a calculated  $\log P$  of 4.11, three hydrogen bond donors, three hydrogen bond acceptors, four rotatable bonds, and three rings. Other diaryltriazines have been reported to have promising anti-HIV activity [42], but the main advantage that compound **18a** has over other compounds with its butterfly structure is that its charged ammonium group is ideally placed to interact strongly with the Glu 138 carboxylic group, and its other ring substitutions, two *p*-toluene groups, are perfectly symmetric. This combination of features is absent from the other compounds.

The binding mode resembles that of the known and approved NNRTI drugs, and it especially resembles those of a different class of compounds, the binding mode of diarylpyrimidine [43] and the approved drugs etravirine [44] and rilpivirine [45]. Moreover, it has been proposed that this particular binding mode has advantages for allowing a strong fit in the tight, closed hydrophobic binding pocket, but that at the same time, the flexibility in the “wings” of compound **18a** could provide it with a degree of adaptability to conformational and mutational change in the protein [42]. The molecular symmetry of **18a** also allows it to bind tightly in a 180° flip, which would increase the number of favorable conformers and binding modes of the protein.

The computational analysis shows that compared to **18a**, compound **18b** has an even stronger interaction with the protein (**Table 3**). Compound **18b** represents a difference of one isosteric substituent with compound **18a**, the replacement of  $-\text{NH}_3^+$  by  $-\text{OH}$ , and they possess the same molar mass and similar polarity. Similarly to **18a**, **18b** also has interactions with protein

such as donating and receiving hydrogen bonds to the backbone NH and CO of Lys 101 using an exocyclic and an endocyclic nitrogen, with **18b** using in addition a hydroxyl group, as shown in **Figure 3**. This change loses the ionic interaction of **18a**, but it gains a slightly deeper binding mode inside the protein binding-site. Such symmetrical compounds have the advantage of being capable of binding to the protein in the same way after a 180° flip.

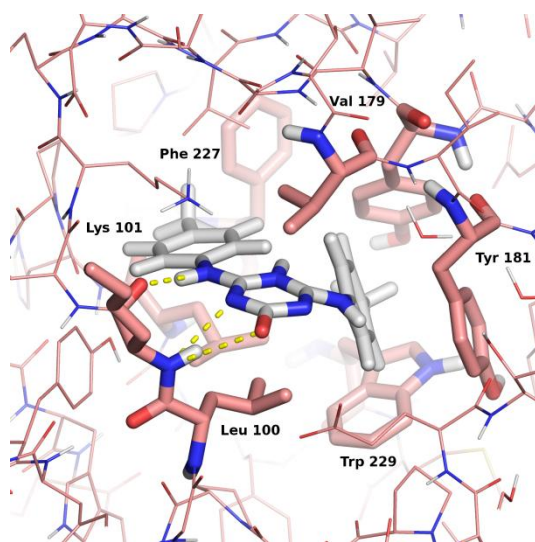


**Figure 3.** Docked binding mode of compound **18b** with the HIV-1 RT crystal structure. Hydrogen atoms are in white, oxygen atoms are in red, and nitrogen atoms are in blue. Ligand carbon atoms are in grey, and protein carbon atoms are in pink. All of the hydrogen atoms are shown for the ligand, and the polar hydrogens are shown for the protein. Compound **18b** donates and accepts three conjugated (close) hydrogen bonds (yellow dashes) from Lys101 backbone atoms, as well as forming deep and enclosed hydrophobic contacts with the sidechains of Phe 227, Tyr181, Tyr 188, Val 179, Trp229, and Leu 100.

Compound **18b** has the same low molecular weight of 307.4 g/mol as **18a**, and three hydrogen bond donors, three hydrogen bond acceptors, four rotatable bonds, three rings, and a moderate, calculated  $\log P$  of 5.16. Compound **18b**, on the other hand, has a slightly deeper binding than compound **18a**; its hydroxyl group can make stronger hydrogen bonds than the amine group in **18a** and has a large number of resonance structures that can stabilize tautomers and protonation states, which could provide its stronger activity. These equivalent states could enhance the binding to the protein. The nitrogen groups on the heterocycle as well as on the side



chains, together with the less polar toluene functional groups, allow a balance in the compound's polarity and solubility properties. Compound **18b** has not been reported in HIV-1 or in any other biological or material research.

The loss of the salt bridge inside the protein can incur a loss of around 4 kcal/mol in the free energy of binding, yet the charged amino group can also have a high desolvation energy, as well as difficulties in membrane transport. The better activity of **18b** compared to **18a** can thus be related to a tighter (deeper) fit in the binding site, the availability of a higher number of resonance structures for **18b**, or stronger hydrogen bonding of OH groups relative to amino groups, as has been reported elsewhere [46]. In addition, the side chain of Glu138 is the hydrogen bond partner of **18a**, whereas **18b** makes all three hydrogen bonds to Lys101 backbone atoms. Since side chains are more dynamic (especially so the flexible side chain of glutamate), it would be expected that the hydrogen bonds to the backbone atoms of Lys101 would be more conserved and easier to maintain than a hydrogen bond to the mobile side chain of Glu138. The actual score breakdowns show a higher Rewards term for **18b** of -38.5 kcal/mol compared to -35.2 kcal/mol for **18a**. The Rewards term in Glide accounts for rewards and penalties to the scoring function for various features, such as buried polar groups, a hydrophobic enclosure, correlated hydrogen bonds, amide twists, among others [47]. The deeper, tighter binding of **18b** compared to **18a** would favor a better burial of polar groups, and better enclosure of the hydrophobic groups from the bulk solvent, and possibly stronger correlated hydrogen bonds (that is, hydrogen bonds at a small distance separation – one or two bonds - from each other).

## 2.5 Cytotoxicity and antiviral activity of novel *s*-triazine derivatives

Toxicity and antiretroviral activity of the synthesised compounds **8** (isomers si1, si2), **17**, **18a**, **18b**, and **19** were analysed. The obtained results were consistent with previously obtained experimental data for sample components (see chapter 2.2) and with computational predictions (see chapter 2.4). It was confirmed that synthesised **8** and its stereoisomers were weak inhibitors of HIV-1 infection. They showed weak activity in experiments with HIV-1-based VLPs and no activity against purified HIV-1 RT in cell-free assay or against infectious HIV-1 in cell culture assay (**Table 2**, see also: **Figure S3: 8(p.)** and **Figure S5**). Consistent with the results obtained for component **19** (**Figure S3**), the synthesised compound **19** also lacked anti-HIV-1 activity (**Table 2**). The same was found to be the case for synthesised compound **17** (**Table 2** and data not shown). This data indicates and confirms that **17** and **19** were not responsible for the anti-HIV-1 activity of the original sample of **8**.

In accordance with *in silico* predictions (see section 2.4), synthesised **18a** was found to be an efficient HIV-1 RT inhibitor. In the assay based on the use of HIV-1 VLPs, the  $IC_{50}$  of **18a** was found to be  $2.5 \pm 0.3 \mu\text{M}$  (**Table 2; Figure S6: A**). The cytotoxic concentration ( $CC_{50}$ , the concentration of the compound that reduces the cell viability by 50%) for U2OS cells was  $42.2 \pm 5.6 \mu\text{M}$ , and the SI (selectivity index, the ratio  $CC_{50}/IC_{50}$ ) was approximately 17. Importantly, comparable values were obtained in the assay using infectious HIV-1 ( $IC_{50} = 5.6 \pm 1.1 \mu\text{M}$ ,  $CC_{50} = 57 \pm 22 \mu\text{M}$  (when measured for TZM-bl cells), and SI was approximately 10 (**Table 2; Figure S6: B**). Expectedly, **18a** also showed a dose-dependent inhibition of purified HIV RT in the cell free assay ( $IC_{50} = 116 \pm 12 \mu\text{M}$ ) (**Table 2, Figure S6: C**). Finally, the anti-HIV-1 effect of **18a** was clearly specific to the wt HIV-1 RT because the compound was not active against

HIV-1 VLPs that contained RT with mutations that are associated with resistance against NNRTIs (**Figure S7**).

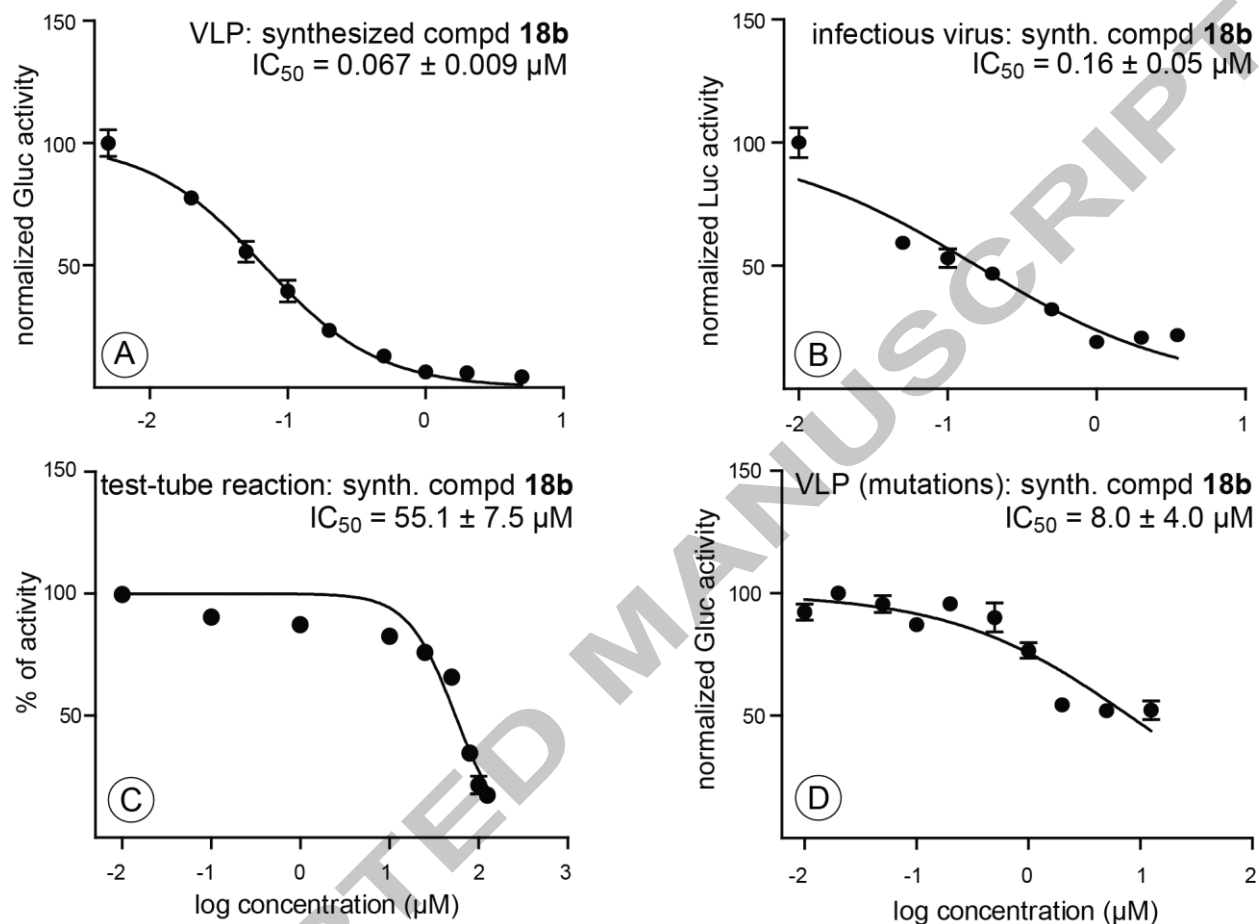


**Figure 4.** Compound **18b** reduces the infectivity of HIV-1 VLPs (**A**) and HIV-1 virions (**B**) in cell-based assays and the activity of HIV-1 RT in the cell-free test-tube reaction (**C**). Compound **18b** also reduces the infectivity of HIV-1 VLPs that contain RT that harbors the K103N and Y181C mutations (**D**). Each experiment was performed in triplicate; DMSO was used as a vehicle control, and the corresponding values were set to 100%. The error bars represent the standard deviation. Data from one reproducible experiment are shown.

Compound **18b** revealed no cytotoxicity at concentrations up to  $12.5 \mu\text{M}$  (data not shown); higher concentrations could not be assayed due to the limited solubility of **18b**. At the same time, **18b** was the most potent HIV-1 inhibitor among all of the tested compounds: in the assay based on the use of HIV-1 VLPs, the  $\text{IC}_{50}$  of **18b** was  $0.067 \pm 0.009 \mu\text{M}$ , which is approximately 5-fold lower than that of the original **8** (n.p.) from stock (**Figure 4: A, Table 2**).

Importantly, similar results (**Figure 4: B, Table 2**) were obtained in the assay in which infectious HIV-1 was used instead of VLPs ( $IC_{50} = 0.16 \pm 0.05 \mu\text{M}$ ). It was also shown (**Figure 4: C, Table 2**) that this compound is active against the purified RT of HIV ( $IC_{50} = 55.1 \pm 7.5 \mu\text{M}$ ). The effect of **18b** was specific for wt HIV-1 RT because the compound had no effect on the HIV-1 VLPs that contained RT with a single K103N or single Y181C mutation (data not shown). However, the compound demonstrated moderate activity (**Figure 4: D**) against HIV-1 VLPs that contained RT with both indicated mutations, although in this case, the calculated  $IC_{50}$  ( $8.0 \pm 4.0 \mu\text{M}$ ) was more than 100-fold higher than in the case in which the VLPs contained wt HIV-1 RT.

Thus, although compound **18a** is less efficient than compound **18b**, they represent novel HIV-1 NNRTI-s. Both compounds have not been reported in HIV or any other biological or material research before. The discovery of **18b** and **18a** allows us to conclude that the *in silico* screen was successful because their chemical motif is also shared with **8** and for both compounds low toxicity was found. The isosteric replacement of  $-\text{NH}_3^+$  by  $-\text{OH}$  was found to be beneficial to HIV inhibitory activity, which can be rationalised based on its molecular properties and interactions. The relative ranking of the compounds as calculated computationally reflects well the experimentally observed trend.

Other 1,3,5-triazines with different substituents have been reported to bind to the ATP binding site of DNA topoisomerase II $\alpha$ , a target protein in cancer [48, 49], and therefore, further tests can be conducted on these compounds to assess and develop them as regards to their inhibition profile and safety, though they appear to have low toxicity. Compound **18b** is non-toxic at up to  $12.5 \mu\text{M}$ , which is its estimated solubility in the current experimental setting, though **18b** is active in the nanomolar range in cells which provides a window of safety for the possible use of this compound.

### 3 Conclusions

On the basis of the earlier multi-objective *in silico* screening and the current work, novel *s*-triazine derivatives are shown to be HIV-1 NNRTIs. For this, the biological properties of the 16 top-ranked compounds (their commercial samples) were investigated. The commercial non-purified sample **8** was shown to be a potent HIV-1 inhibitor, although it was discovered that closely related compounds that share the *s*-triazine and some of the functional groups were present in the initial commercial preparation and had a strong anti-HIV-1 effect at low concentrations. Iterative and systematic work was performed in the virological, synthetical, analytical, and computational analysis of the data. Altogether, five compounds were synthesised and analysed for their antiviral activity: **8** (its 2 stereoisomers), **17**, **18a**, **18b**, and **19**. The latter four were not available commercially and showed different biological activity. All of them possess a *s*-triazine core and similar functional group substituents. The difference between the strongest inhibitors, **18a** and **18b**, was one conserved functional group:  $-\text{NH}_3^+$  vs.  $-\text{OH}$ , respectively. The most potent, **18b**, exists in several tautomeric forms that can be stabilised through resonance. The compounds proved to be non-toxic and effective in both cell-based and enzyme experiments; the *in silico* methods and systematic follow-up were able to identify a novel group of non-toxic compounds and a new chemotype (1,3,5-triazinone/*s*-triazinone/1,3,5-triazinol/*s*-triazinol) that has the ability to bind to HIV-RT in the NNRTI site and inhibit HIV infectivity. Their binding mode and interactions with the protein suggest strong binding in a tight (NNRTI) hydrophobic pocket, using hydrogen bonds, hydrophobic contacts and  $\pi$ - $\pi$  interactions. Their molecular symmetry affords them with at least two potent binding poses that are equally strong, and their wing-type structure provides adaptability to protein conformational movement. Resonance structures can stabilise the binding modes to the protein. Their small molecular size,

potent ligand efficiencies, and measured low toxicities permit further exploration of their derivatives and the NNRTI binding site. It is also interesting to emphasise that compounds with different degrees of activity can be among the components of commercial samples and that computations and a systematic approach can provide valuable clues toward them.

ACCEPTED MANUSCRIPT

## 4 Materials and Methods

### 4.1 *In silico* screened and selected compounds

Samples for 16 compounds of the top thirty compounds from the multi-objective screening and ranking described previously [13] were available commercially. They formed a library for the experimental testing. The compounds were diverse (structures shown in **Figure 1**) as measured by Tanimoto similarity coefficients (mean = 0.24, median = 0.21) that compare the amount of structural commonalities between two compounds. They also had good ligand efficiencies ( $\Delta G/PSA$  deeper than  $-0.07 \text{ kcal}/(\text{mol}\cdot\text{\AA}^2)$  [13],  $\Delta G/MW$  deeper than  $-0.02 \text{ (kcal}\cdot\text{g)}/\text{mol}^2$  [13], and  $\Delta G/NHA$  deeper than  $-0.24 \text{ kcal}/(\text{mol}\cdot\text{NHA})$  [50]). The ligand efficiencies normalise the binding energy of a compound by a factor that can be related to the size or other physicochemical features of the compound. This initial set included quinolin-2-ones, chromen-2-ones, purines, and related rings that are present among the top-ranked compounds. Nitrogen compounds also featured prominently. Compounds **14** and **15** were different protonation states in the *in silico* screen, although they were tested experimentally with the same compound.

### 4.2 *Computational methods*

Chemical compounds were drawn and energy minimised with MacroModel version 9.9 [51]. Protein X-ray crystal structures were assigned polar hydrogen atoms and prepared (including energy minimisation) using the Protein Preparation Wizard version 1.0 [52]. Docking was conducted using Glide version 5.9 [47] with rigid protein and fully flexible ligand structures, scoring with XP GlideScore.  $\text{Log}P$  was calculated with the program xlogP3.0 [53].

### 4.3 Chemical synthesis

#### 4.3.1 Chemicals.

Samples of **1**, **7**, **11**, **13**, and **14** were purchased from Vitas-M Laboratory, Ltd.; samples of **2**, **4**, **5**, **6**, and **16** from Enamine Ltd.; samples of **3** and **12** from InterBioScreen Ltd.; a sample of **9** from Asinex Ltd.; and a sample of **10** from Otava Ltd. Samples of **8** were purchased from both InterBioScreen Ltd. and ChemBridge Corporation, and these samples were equivalent in composition and behaviour.

Other solvents and reagents were obtained commercially and used without further purification. The 2,4,6-trisubstitued-pyrimidine derivatives (**8**, **17**, **18a**, **18b** and **19**) were synthesised from 2,4,6-trichloro-1,3,5-triazine, by sequential substitution of the chloride atom using oxygen and nitrogen centered nucleophiles. In general, the first chlorine was displaced at a temperature of 0 °C or below, and the second chlorine was displaced at room temperature (between 22 °C and 26 °C); the third chlorine was displaced with a temperature between 80 °C and 90 °C. All of the substituted derivatives were purified by column chromatography using different eluents (specified in the methods section). The reaction sequence is given in **Scheme 1**. All of the synthesised compounds were fully characterised by spectroscopic data obtained by HPLC-DAD, MS (high-resolution ESI-QTOF and ESI-FT-ICR-MS) and NMR.

#### 4.3.2 2-N,4-N-bis(4-methylphenyl)-6-N-(oxolan-2-ylmethyl)-1,3,5-triazine-2,4,6-triamine (**8**)

A solution of cyanuric chloride (5.05 g, 27.33 mmol) in anhydrous dichloromethane (50 mL) was added *via cannula* (dropwise, 6 min.) to a stirred solution of *p*-toluidine (2 eq) and diisopropylamine (2.85 eq) in anhydrous dichloromethane (60 mL) at 0 °C under argon. Then, the reaction mixture was allowed to reach room temperature. After 14 h, the mixture was partitioned between CH<sub>2</sub>Cl<sub>2</sub> (40 mL) and the saturated aqueous sodium chloride (60 mL), and the



combined organic layers were dried with  $\text{MgSO}_4$ , filtered, evaporated to dryness and purified by flash chromatography (dichloromethane/diethyl ether 4:1) to afford **8(I)** a 97 % yield.

Compound **8(I)** (3.72 g, 11.42 mmol) and tetrahydrofuran-4-amine (1.5 eq) were dissolved in dioxane (20 mL) under argon, and the reaction mixture was refluxed for 21 h. The solvent was evaporated *in vacuo*, and the residue was purified with flash chromatography (dichloromethane/ethyl acetate 1:1) to afford compound **8** a 93 % yield. The parameters that were relevant are the following:  $^1\text{H}$  NMR ( $\text{CDCl}_3$ ,  $+50^\circ\text{C}$ , 700 MHz)  $\delta$ : 7.44 (AA' part of AA' BB' multiplet, 4H,  $4\times\text{CH}_{\text{ar}}$ ); 7.10 (BB' part of AA' BB' multiplet, 4H,  $4\times\text{CH}_{\text{ar}}$ ); 6.95 (br. s, 2H,  $2\times\text{PhNH}$ ); 5.76 (br. s, 1H,  $\text{CH}_2\text{NH}$ ); 4.08 (dddd,  $J=6.9, 6.5, 6.3, 3.9$  Hz, 1H,  $\text{CH-O}$ ); 3.90 (ddd,  $J=8.4, 7.2, 6.2$  Hz, 1H,  $\text{CH}_{2\text{a-O}}$ ); 3.77 (ddd,  $J=8.4, 7.4, 6.3$  Hz, 1H,  $\text{CH}_{2\text{b-O}}$ ); 3.67 (ddd,  $J=13.8, 6.3, 3.9$  Hz, 1H,  $\text{CH}_{2\text{a-N}}$ ); 3.47 (ddd,  $J=13.8, 6.5, 5.7$  Hz, 1H,  $\text{CH}_{2\text{b-N}}$ ); 2.33 (m, 6H,  $2\times\text{CH}_3$ ); 1.99 (dddd,  $J=12.2, 8.5, 6.9, 5.3, 0.4$  Hz, 1H  $\text{CH}_{2\text{a-C}}$ ); 1.91 (m, 2H,  $2\times\text{CH}_{2\text{b-C}}$ ); 1.65 (dddd,  $J=12.2, 8.8, 7.4, 7.2, 0.5$  Hz, 1H,  $\text{CH}_{2\text{a-C}}$ );  $^{13}\text{C}$  NMR ( $\text{CDCl}_3$ ,  $+50^\circ\text{C}$ , 176 MHz)  $\delta$ : 166.3; 164.4; 136.4; 132.6; 129.2; 120.8; 78.0; 68.1; 44.6; 28.7; 25.9; 20.7; HRMS (ESI)  $m/z$  391.22393  $[\text{M}+\text{H}]^+$  ( $\text{C}_{22}\text{H}_{27}\text{ON}_6^+$  requires 391.22409).

#### 4.3.3 2-N-(4-methylphenyl)-4-N,6-N-bis(oxolan-2-ylmethyl)-1,3,5-triazine-2,4,6-triamine (17)

A solution of cyanuric chloride (2.14 g, 10.93 mmol) in anhydrous dichloromethane (20 mL) was added *via cannula* (6 min) to a stirred solution of tetrahydrofuran-4-amine (2 eq) and diisopropylamine (2.85 eq) in anhydrous dichloromethane (40 mL) at  $0^\circ\text{C}$  under argon, and the reaction mixture was allowed to warm to room temperature. After 14 h, the mixture was partitioned between  $\text{CH}_2\text{Cl}_2$  (30 mL) and the saturated aqueous sodium chloride (60 mL). The combined organic layers were dried with  $\text{MgSO}_4$ , filtered, evaporated to dryness and purified by flash chromatography (ethyl acetate/hexane 9:1) to afford compound **17(I)** a 61 % yield.

A mixture of compound **17(I)** (2.09 g, 6.68 mmol) and *p*-toluene (1.5 eq) in dioxane (26 mL) under argon was refluxed for 21 h. The solvent was evaporated *in vacuo*, and the residue was purified with flash chromatography (acetonitrile/methanol 1:0.1) to afford compound **17** an 89 % yield. The parameters that were relevant are the following:  $^1\text{H}$  NMR ( $\text{CDCl}_3$ , +50 °C, 700 MHz)  $\delta$ : 7.44 (AA' part of AA' BB' multiplet, 4H,  $4\times\text{CH}_{\text{ar}}$ ); 7.08 (BB' part of AA'BB' multiplet, 4H,  $4\times\text{CH}_{\text{ar}}$ ); 6.9 (br. s, 1H,  $\text{PhNH}$ ); 5.47 (br. s, 2H,  $2\times\text{CH}_2\text{NH}$ ); 4.05 (dddd,  $J=7.0$ , 6.8, 6.7, 4.1 Hz, 2H,  $\text{CH-O}$ ); 3.89 (ddd,  $J=8.4$ , 7.2, 6.1 Hz, 2H,  $\text{CH}_{2\text{a-O}}$ ); 3.75 (ddd,  $J=8.4$ , 7.6, 6.3 Hz, 2H,  $\text{CH}_{2\text{b-O}}$ ); 3.61 (m, 2H,  $\text{CH}_{2\text{a-N}}$ ); 3.44 (m, 2H,  $\text{CH}_{2\text{b-N}}$ ); 2.31 (m, 6H,  $2\times\text{CH}_3$ ); 1.93 (m, 4H,  $2\times\text{CH}_3$ ,  $2\times\text{CH}_{2\text{a-C}}$ ); 1.63 (m, 4H,  $2\times\text{CH}_{2\text{b-C}}$ ,  $2\times\text{CH}_{2\text{a-C}}$ );  $^{13}\text{C}$  NMR ( $\text{CDCl}_3$ , +50 °C, 176 MHz)  $\delta$ : 166.0; 164.1; 136.7; 132.2; 129.1; 120.3; 77.9; 77.2; 77.0; 76.8; 68.1; 44.5; 28.7; 25.9; 20.7; HRMS (ESI)  $m/z$  385.23414  $[\text{M}+\text{H}]^+$  ( $\text{C}_{20}\text{H}_{29}\text{O}_2\text{N}_6^+$  requires 385.23465).

#### 4.3.4 2-*N*-hydroxy-4-*N*,6-*N*-bis(4-methylphenyl)-1,3,5-triazine-2,4,6-triamine (**18a**)

To a stirred solution of cyanuric chloride (2.16 g, 11.69 mmol) in anhydrous dichloromethane (10 mL) ammonium hydroxide (1 eq) was added dropwise. The residue was purified with flash chromatography (ethyl acetate/dichloromethane 8:2) to afford compound **18(I)** a 99% yield.

*p*-toluene (2.5 eq) was added under argon to a stirred solution of compound **18(I)** (4 g, 24.25 mmol) in dioxane (80 mL). The reaction mixture was stirred for 20 h. The residue was purified with flash chromatography (dichloromethane/methanol 1:0.1) to afford compound **18a** a 71 % yield. The parameters that were relevant are the following:  $^1\text{H}$  NMR ( $\text{DMSO-}d_6$ , +50 °C, 700 MHz)  $\delta$ : 9.72 (br. s, 2H,  $2\times\text{NH}$ ); 7.54 (AA' part of AA' BB' multiplet, 4H,  $4\times\text{CH}_{\text{ar}}$ ); 7.45 (br. s, 2H,  $\text{NH}_2$ ); 7.11 (BB' part of AA'BB' multiplet, 4H,  $4\times\text{CH}_{\text{ar}}$ ); 2.28 (s, 6H,  $2\times\text{CH}_3$ );  $^{13}\text{C}$  NMR ( $\text{DMSO-}d_6$ , +20 °C, 176 MHz)  $\delta$ : 160.9; 135.9; 132.5; 129.0; 121.3; 40.0; 39.9; 39.7; 39.6;

39.5; 39.4; 39.3; 39.2; 20.5; HRMS (ESI)  $m/z$  307.16661  $[M+H]^+$  ( $C_{17}H_{19}N_6^+$  requires 307.16657).

#### 4.3.5 2-N,4-N,6-N-tris(4-methylphenyl)-1,3,5-triazine-2,4,6-triamine (**19**)

A stirred solution of compound **8(I)** (2.01 g, 10.93 mmol) and *p*-toluidine (1.5 eq) in dioxane (25 mL) under argon was refluxed for 21 h. The solvent was evaporated *in vacuo*, and the residue was purified with flash chromatography (dichloromethane/*n*-hexane/methanol 5:5:01) to afford compound **19** a 98% yield. The parameters that were relevant are the following:  $^1H$  NMR (DMSO- $d_6$ , +50 °C, 700 MHz)  $\delta$ : 7.35 (AA' part of AA' BB' multiplet, 4H, 4 $\times$ CH<sub>ar</sub>); 7.03 (BB' part of AA'BB' multiplet, 4H, 4 $\times$ CH<sub>ar</sub>); 6.86 (br. s, 3H, 3 $\times$ NH); 2.25 (m, 9H, 3 $\times$ CH<sub>3</sub>);  $^{13}C$  NMR (CDCl<sub>3</sub>, +50 °C, 176 MHz)  $\delta$ : 164.6; 136.2; 133.2; 129.5; 121.2; 77.3; 77.2; 76.9; 20.9; HRMS (ESI)  $m/z$  397.21353  $[M+H]^+$  ( $C_{24}H_{25}N_6^+$  requires 397.21352).

#### 4.3.6 Bis[(4-methylphenyl)amino]-1,3,5-triazine-2-ol a.k.a. 4,6-bis[(4-methylphenyl)amino]-1H-1,3,5-triazin-2-one a.k.a. 4,6-bis[(4-methylphenyl)amino]-5H-1,3,5-triazin-2-one (**18b**)

The mixture of distilled H<sub>2</sub>O (42 mL) and TFA (0.5 eq) was added to compound **8(I)** (350 mg, 1.07 mmol) in the reaction vessel. The reaction mixture was refluxed for 120 h, evaporated to dryness and purified by recrystallisation from ethanol to afford compound **18b** with 60 % yield. The following data was measured for the synthesised comp **18b**:  $^1H$  NMR (DMSO- $d_6$ , +50 °C, 700 MHz)  $\delta$ : 7.70 (AA' part of AA' BB' multiplet, 4H, 4 $\times$ CH<sub>ar</sub>); 7.05 (BB' part of AA'BB' multiplet, 4H, 4 $\times$ CH<sub>ar</sub>); 3.23 (br. s, 3H, 3 $\times$ NH); 2.61 (br. d,  $J=9.6$  Hz, 18H, 6 $\times$ CH<sub>3</sub> phosphazene); 2.26 (s, 6H, 2 $\times$ Ph-CH<sub>3</sub>); 1.18 (br. s, 9H, C-CH<sub>3</sub>)<sub>3</sub> phosphazene);  $^{13}C$  NMR (DMSO- $d_6$ , +50 °C, 176 MHz)  $\delta$ : 165.91; 163.86; 138.7; 129.0; 120.3; 49.2; 40.5; 40.4; 40.2; 40.1; 40.0; 39.89, 39.77; 39.90; 36.90; 36.88, 29.8; 20.8; HRMS (ESI)  $m/z$  308.15057  $[M+H]^+$  ( $C_{17}H_{18}ON_5^+$  requires 308.15059).

#### 4.4 *Materials and instruments.*

All of the final compounds were purified to >95% by column chromatography, using Silica gel 40 MN (Fluka -60735, particle size 0.063-0.2 mm, 70-230 mesh ASTM) and aluminium backed Silica gel 60 F<sub>254</sub> from Merck was used for analytical TLC. Mass spectra (MS) were obtained from the Mass Spectrometry Voyager DE Pro (Applied Biosystems, USA).

<sup>1</sup>H and <sup>13</sup>C NMR measurements were conducted using either Bruker AVANCE III 700 (700.1 MHz for <sup>1</sup>H and 176.1 MHz for <sup>13</sup>C) or Bruker AVANCE 500 (500.1 MHz for <sup>1</sup>H and 125.8 MHz for <sup>13</sup>C) instruments at +20 or + 50 °C. The higher temperature was used to make the rate of the tautomeric equilibrium faster and therefore to obtain sharper signals in the spectra. <sup>1</sup>H chemical shifts were directly referenced to internal TMS (0.00 ppm) or indirectly to TMS via the solvent signal (CHCl<sub>3</sub>, 7.26 ppm, DMSO-*d*<sub>5</sub>, 2.50 ppm), and <sup>13</sup>C chemical shifts were indirectly referenced to TMS via the solvent signal (CDCl<sub>3</sub>, 77.00 ppm, DMSO-*d*<sub>6</sub>, 39.52 ppm).

Sample analysis was performed with the Shimadzu LC Solution (Prominence) system by using an injector and a diode array detector (SPD 20A) with a mass detector (LCMS 2020). Separation was achieved with a Gemini C18 5µm column (250×4.6 mm i.d., Phenomenex) protected by a 5µm Gemini C18 guard column (4×2.0 mm i.d., Phenomenex). Mobile phase A: 0.1 % TFA, mobile phase B: 0.1 % TFA in ACN and a flow rate of 1 mL/min were employed. The linear gradient speed was 3 % B/min, and elution was started at 3 min (the injection time was also at 3 min) with 30 % B. Sample peaks were confirmed by the retention time and mass data. Electrospray ionization was achieved at a positive mode for [M+H]<sup>+</sup>. The desolvation line temperature was 250 °C, the heat block temperature 200 °C, the ionization voltage 4.5 kV, and the qarray RF voltage 60 V. The drying gas flow was set at 15 L/min and the drying gas temperature at 250 °C; the scan speed was 15,000 µ/sec.

The mixture **17/18** was analysed by Agilent's 1200 series HPLC combined with a diode array detector and microTOF<sub>Q</sub> mass spectrometer (Bruker Daltonics), i.e., by HPLC-ESI-QTOF-MS. Separation was achieved by a BEHC18 column (Acquity UPLC, Waters) with a gradient elution. Two mobile phases, A: ACN and B: 0.1 % HCOOH, were used as follows: 0-5 min 0-30 % A in B, 5-6 min 30-70 % A in B, and 6-8 min 70 % A in B. The flow rate was 0.45 mL/min, and the injection volume was 5  $\mu$ L. Electrospray ionization was used in a positive ion mode. The capillary voltage was set at -4500 V, with the end plate offset at -500 V. The nebulizer gas (N<sub>2</sub>) was set at 1.6 bar, and the dry gas (N<sub>2</sub>) flow was set at 8 L/min and the temperature at 200 °C. A mass range of  $m/z$  50–3000 was used. The data were handled by Bruker Compass DataAnalysis (version 4.0).

High-resolution ESI-ICR spectra were obtained on a hybrid Varian 910-FT-ICR-MS system, which was coupled to Varian-J320 triple-quadrupole MS. The ionization parameters were as follows: ESI-needle voltage, 5000 V; spray chamber temperature, 40°C; nebulizing gas (N<sub>2</sub>) pressure, 30 psi at 300 °C; API-drying gas (N<sub>2</sub>), 18 psi at 300 °C; shield voltage, 600 V; and capillary voltage, 60 V; and infusion rate, 10  $\mu$ L/min. The ion guide and FT-ICR parameters were optimised for the mass range  $m/z$  100–800 as described in ref. [54]. The ion collection time was 500 ms, after which ions were passed to the FT-ICR analyser cell for excitation and detection (detection mode: direct (broadband); ADC rate: 4 MHz; transient length: 2048 K; 524.288 ms). Samples were dissolved in 1 % HCOOH MeOH solution, so that final concentration of analyte was about 10  $\mu$ g/ml. For steady calibration of the  $m/z$  axis, samples were spiked with the in-house prepared internal calibration solution, which contained ions with the following exact  $m/z$  values: 1. C<sub>16</sub>H<sub>36</sub>N<sup>+</sup> ( $m/z$  = 242.28423); C<sub>19</sub>H<sub>29</sub>N<sub>4</sub>PF<sub>3</sub><sup>+</sup> ( $m/z$  = 401.20765) [55]; 3. C<sub>26</sub>H<sub>45</sub>N<sub>7</sub>P<sub>2</sub>Cl<sup>+</sup>

( $m/z = 552.28947$ ) [55]; 4.  $C_{26}H_{64}N_{13}P_4^+$  ( $m/z = 682.43526$ ) [56]. The concentration of the calibrants in the infused solutions remained within range 0.5–1.0 mM.

#### 4.5 *Cell-culture based assays used for cytotoxicity and anti-HIV-1 activity measurements*

##### 4.5.1 *Materials used.*

Dimethyl sulfoxide (DMSO), polybrene, Phorbol 12-myristate 13-acetate (PMA), nevirapine and trichloroacetic acid (TCA) were purchased from Sigma Aldrich (USA).  $Na_4P_2O_7$  was purchased from Applichem (Germany). Recombinant purified HIV-1 reverse transcriptase was purchased from Calbiochem (USA).

##### 4.5.2 *Cells and growth media.*

ACH-2 and TZM-bl cell lines were obtained through the NIH AIDS Reagent Program, Division of AIDS, NIAID, NIH: ACH-2 [57,58] from Dr. Thomas Folks and TZM-bl [59,60,61,62,63] from Dr. John C. Kappes, Dr. Xiaoyun Wu and Tranzyme Inc.

U2OS human osteosarcoma cells were obtained from ATCC and grown in Iscove's Modified Dulbecco's Medium (IMDM) supplemented with 10 % fetal bovine serum (FBS), 100 U Penicillin and 100  $\mu\text{g}/\text{mL}$  Streptomycin (Pen/Strep). ACH-2 cells were grown in Roswell Park Memorial Institute medium 1640 (RPMI 1640) supplemented with 25 mM HEPES, 0.3 g/L L-Glutamine, 10 % heat-inactivated FBS and Pen/Strep. TZM-bl cells were grown in Dulbecco's Modified Eagle's medium (DMEM) supplemented with 10 % heat-inactivated FBS and Pen/Strep. All of the cells were grown at 37 °C in the presence of 5 %  $CO_2$ . All of the reagents and media used for cell cultivation were purchased from Naxo OÜ (Estonia).

##### 4.5.3 *Cytotoxicity assay.*

The cytotoxicity of compounds **1-19** was measured using the xCELLigence RTCA DP Instrument (ACEA Biosciences, Inc) as follows.  $3.5 \times 10^3$  U2OS cells or  $8.5 \times 10^3$  TZM-bl cells

were seeded per well of E-plate 16 (ACEA Biosciences, Inc) with micro-electrodes integrated on the bottom. Then, 24 hours later, compounds dissolved in DMSO were added. The final concentration of DMSO was kept constant (0.5 %) in all of the used media, and the media that contained the same amount of DMSO with no compound added was used as the vehicle control. Cells were incubated for an additional 48 hours, and the impedance signals between the electrodes were recorded for all of this period. The concentration of the compound was considered to be toxic if it reduced the cell index by more than 50 % in comparison to cells that were treated with only DMSO; the concentration of the compound was considered to be moderately toxic if it reduced the cell index by 20-50 %; and concentration of the compound was considered to be non-toxic if the cell index was reduced by no more than 20 %.

#### 4.5.4 *Production of the HIV-1 stock.*

Here,  $6 \times 10^6$  ACH-2 cells were seeded in 10 mL of full culture media, and HIV-1 production was induced by the addition of 100 nM PMA. The induced cells were incubated for 48 hours, and subsequently, the HIV-1 containing media was collected. The amount of HIV-1 p24 protein that was released into the media was measured using anti p24-ELISA, which was developed in-house; this approach was used to estimate the titer of the obtained virus stocks.

#### 4.5.5 *Analysis of the antiviral activity of compounds using HIV-1 VLPs.*

HIV-1 based VLPs were obtained using ViraPower Lentiviral Expression System according to the manufacturer's (Invitrogen) instructions. The RNA packed into the VLPs was engineered to contain the *Gaussia* luciferease (Gluc) encoding region, in such a way that upon reverse transcription and integration of the resulting cDNA into the cell genome, the marker protein would be expressed from transcripts made using the human cytomegalovirus early promoter. Mutations K103N, Y181C or double mutation K103N/Y181C of HIV-1 RT, which are known to

result in nevirapine-resistant HIV-1 genotypes [64], were introduced into the reverse transcriptase gene of HIV-1 using site-directed mutagenesis. VLPs that contained enzymes with such mutations were obtained as described above.

For the analysis of the antiviral activities of the compounds, the U2OS cells were seeded on a 24-well plate at a density of  $5 \times 10^4$  cells per well. The next day, the cells were infected with HIV-1 VLPs that contained wt or mutant reverse transcriptase at a multiplicity of infection (MOI) = 0.01 infectious units/cell in the presence of polybrene 6  $\mu\text{g}/\text{mL}$  and the analysed compounds or nevirapine (positive control) at the indicated concentrations; media that contained 0.5% DMSO was used as a vehicle control. The cells were incubated with VLPs for 1 hour (37 °C, 5 %  $\text{CO}_2$ ), and subsequently, they were washed, and full media that contained the indicated amounts of the analysed compounds was added. Incubation was continued for 24 hours, and subsequently, the media was replaced with fresh media that lacked the analysed compounds, and incubation was continued for another 24 hours. Afterward, the cells were lysed, and the Gluc activity in the cells was measured using *Renilla* Luciferase Assay System and Glomax 20/20 Luminometer (Promega). The protein concentration in the cell lysates was measured using the Bio-Rad protein assay, and the Gluc activity was normalised to the protein concentration.

#### 4.5.6 Antiviral assay using HIV-1 virions.

TZM-bl cells contain gene encoding for firefly luciferase (Luc) marker under control of HIV-1 LTR promoter. The expression of this marker is activated by the tat-protein produced by integrated HIV-1 provirus [62,63,65]. In this assay, TZM-bl cells were seeded on a 24-well plate ( $5 \times 10^4$  cells per well). The next day, the cells were infected with HIV-1 stock (media that contained 30 ng of HIV-1 p24 was used per well) in the presence of the indicated amounts of the analysed compounds; nevirapine was used as a positive control, and 0.5 % DMSO was used as a



vehicle control. The cells were first incubated with 150  $\mu$ L of infectious media for 2 hours (37  $^{\circ}$ C, 5 %  $\text{CO}_2$ ). Then, the infectious media was replaced with 1 mL of full growth media that contained the indicated amounts of the compounds or controls; the incubation was continued for 48 hours. Subsequently, the cells were lysed, and Luc activity was measured using the Luciferase Assay System and Glomax 20/20 Luminometer (Promega). The protein concentration in the cell lysates was measured using the Bio-Rad protein assay, and the Luc activity was normalised to the protein concentration.

#### 4.5.7 Inhibition of the DNA polymerase activity of HIV-1 RT.

In a cell-free assay, a 234-nt long RNA (fragment of *Renilla* luciferase mRNA) was used as a template; an 18-mer DNA oligonucleotide, complementary to the 3'-end of the RNA template, was used as a primer. First, the template and primer were mixed at a 1:2 molar ratio in buffer A (10 mM Tris-HCl, pH 7.5, 1 mM EDTA), heated for 2 minutes at 95  $^{\circ}$ C and annealed by cooling for 10 minutes on ice. The subsequent assay was performed in a final volume of 25  $\mu$ L. The reaction mixture contained buffer R (50 mM Tris-HCl, pH 7.8, 1 mM DTT, 6 mM  $\text{MgCl}_2$ , 80 mM KCl, 0.3 % PEG 4000), 50  $\mu$ M of dATP, dGTP and dTTP, 5  $\mu$ M dCTP, 1 unit of recombinant purified HIV-1 RT (Calbiochem) and 1  $\mu$ Ci (0.33 pmol)  $\alpha$ [ $\text{P}^{33}$ ]dCTP (Perkin Elmer). The tested compounds were added in the indicated amounts, and nevirapine was used as a positive control. The final concentration of DMSO in all of the reaction mixtures was 5 %, and the same amount of DMSO was used as a vehicle control. RT and all of the components of the reaction (except template-primer) were pre-incubated together for 15 minutes at room temperature, and then, the reaction was started by the addition of the annealed template-primer (4 pmol primer: 2 pmol template). Mixtures were incubated for 40 minutes at 37  $^{\circ}$ C. Then, 1 mL of solution B (10 % TCA, 0.5 %  $\text{Na}_4\text{P}_2\text{O}_7$ ) and 100  $\mu$ g of salmon sperm carrier DNA were added,

mixed and incubated on ice for 30 minutes. Afterward, the samples were filtered through a GF/C Whatman filter and washed twice with 5 mL W solution (1 % TCA, 0,1 %  $\text{Na}_4\text{P}_2\text{O}_7$ ). The filters were dried, 5 mL of scintillation cocktail ScintiSafe 3 (Fisher Scientific) was added, and the radioactivity bound to the filter was measured with Liquid Scintillation Analyzer Tri-Carb 2810 TR (Perkin Elmer).

#### 4.5.8 *IC50 calculation*

These calculations were performed using GraphPad Prism 5 software (GraphPad Software, Inc).

ACCEPTED MANUSCRIPT

## 5 Acknowledgments

B.V., A.T.G.-S., U.M. and A.M are grateful for their financial support from the Estonian Ministry of Education and Research (grants IUT34-14 and IUT20-27). A.S. and A.M. acknowledge funding from the European Union through the European Regional Development Fund, through the Center of Excellence in Chemical Biology, Estonia. B.V., A.T.G.-S. and U.M., from the Institute of Chemistry, Univ. Tartu, are grateful for help with the analytical instruments from Dr. Gerda-Johanna Raidaru for running and helping with Shimadzu LC Solution (Prominence) with LCMS2020; Dr. Lauri Toom for running and helping with Bruker AVANCE III 700 (Estonian Magnet Laboratory, Tartu Branch); Tõiv Haljasorg for the ESI-HRMS measurements on the Varian 910-FT-ICR-MS system. The Varian 910-FT-ICR-MS system is supported by the Estonian national R & D infrastructure development program Measure 2.3 “Promotion of development activities and innovation” (Regulation No. 34), which is funded by the Enterprise Estonia Foundation.

**6 Supplementary data**

Figures S1 to S7 and Table S1 show the experimental results, followed by the, HPLC, MS and  $^1\text{H}$  and  $^{13}\text{C}$  NMR spectra for the synthesised compounds: **8**, **17**, **18a**, **18b** and **19**.

ACCEPTED MANUSCRIPT

## 7 References

- [1] WHO <http://www.who.int/hiv/data/en/> Accessed on 16th October 2015
- [2] M.-P. de Béthune, Non-Nucleoside Reverse Transcriptase Inhibitors (NNRTIs), Their Discovery, Development, and Use in the Treatment of HIV-1 Infection: A Review of the Last 20 Years (1989-2009), *Antiviral Res.* 85 (2010) 75–90.
- [3] T. Miyasaka, H. Tanaka, M. Baba, H. Hayakawa, R.T. Walker, J. Balzarini, E. De Clercq, A novel lead for specific anti-HIV-1 agents: 1-[(2-hydroxyethoxy)methyl]-6-(phenylthio)thymine, *J. Med. Chem.* 32 (1989), 2507–2509.
- [4] J. Heeres; P.J. Lewi, The Medicinal Chemistry Of The DATA And DAPY Series of HIV-1 Non-Nucleoside Reverse Transcriptase Inhibitors (NNRTIs), in: E. De Clercq (Ed.), *Book Series: Advances in Antiviral Drug Design*, Vol. 5, 2007, pp. 213-242.
- [5] M.L. Barreca, L. de Luca, N. Iraci, A. Rao, S. Ferro, G. Maga, A. Chimirri, Structure-Based Pharmacophore Identification of New Chemical Scaffolds as Non-Nucleoside Reverse Transcriptase Inhibitors. *J. Chem. Inf. Model.* 47 (2007) 557–562.
- [6] G. Barreiro, J.T. Kim, C.R.W. Guimarães, C.M. Bailey, R.A. Domaoal, L. Wang, K.S. Anderson, W.L. Jorgensen, From Docking False-Positive to Active Anti-HIV Agent. *J. Med. Chem.* 50 (2007) 5324–5329.
- [7] A. Herschhorn, A. Hizi, Virtual Screening, Identification, and Biochemical Characterization of Novel Inhibitors of the Reverse Transcriptase of Human Immunodeficiency Virus Type-1. *J. Med. Chem.* 51 (2008) 5702–5713.
- [8] S.E. Nichols, R.A. Domaoal, V.V. Thakur, J. Tirado-Rives, K.S. Anderson, W.L. Jorgensen, Discovery of Wild-Type and Y181C Mutant Non-Nucleoside HIV-1 Reverse Transcriptase Inhibitors Using Virtual Screening with Multiple Protein Structures. *J. Chem. Inf. Model.* 49 (2009) 1272–1279.
- [9] Y. Bustanji, I.M. Al-Masri, A. Qasem, A.G. Al-Bakri, M.O. Taha, In Silico Screening for Non-Nucleoside HIV-1 Reverse Transcriptase Inhibitors Using Physicochemical Filters and High-Throughput Docking Followed by in Vitro Evaluation. *Chem. Biol. Drug Des.* 74 (2009) 258–265.
- [10] S. Distinto, F. Esposito, J. Kirchmair, M.C. Cardia, M. Gaspari, E. Maccioni, S. Alcaro, P. Markt, G. Wolber, L. Zinzula, E. Tramontano, Identification of HIV-1 Reverse Transcriptase Dual Inhibitors by a Combined Shape-, 2D-Fingerprint- and Pharmacophore-Based Virtual Screening Approach. *Eur. J. Med. Chem.* 50 (2012) 216–229.
- [11] A. Ivetac, S.E. Swift, P.L. Boyer, A. Diaz, J. Naughton, J.A.T. Young, S.H. Hughes, J.A. McCammon, Discovery of Novel Inhibitors of HIV-1 Reverse Transcriptase Through Virtual Screening of Experimental and Theoretical Ensembles. *Chem. Biol. Drug Des.* 83 (2014) 521–531.
- [12] H.Q. Wu, Z.H. Yan, W.X. Chen, Q.Q. He, F.E. Chen, E. De Clercq, J. Balzarini, D. Daelemans, C. Pannecouque Towards new C6-rigid S-DABO HIV-1 reverse transcriptase inhibitors: synthesis, biological investigation and molecular modeling studies. *Bioorg. Med. Chem.* 21 (2013) 6477–6483.

- [13] A.T. García-Sosa, S. Sild, K. Takkis, U. Maran, Combined Approach Using Ligand Efficiency, Cross-Docking, and Antitarget Hits for Wild-Type and Drug-Resistant Y181C HIV-1 Reverse Transcriptase. *J. Chem. Inf. Model.* 51 (2011) 2595–2611.
- [14] I.D. Kuntz, K. Chen, K.A. Sharp, P.A. Kollman, The Maximal Affinity of Ligands. *Proc. Natl. Acad. Sci. U. S. A.* 96 (1999) 9997–10002.
- [15] A.L. Hopkins, C.R. Groom, A. Alex, Ligand Efficiency: A Useful Metric for Lead Selection. *Drug Discov. Today* 9 (2004) 430–431.
- [16] A.T. García-Sosa, C. Hetény, U. Maran, Drug Efficiency Indices for Improvement of Molecular Docking Scoring Functions. *J. Comput. Chem.* 31 (2010) 174–184.
- [17] A.T. García-Sosa, U. Maran, C. Hetenyi, Molecular Property Filters Describing Pharmacokinetics and Drug Binding. *Curr. Med. Chem.* 19 (2012) 1646–1662.
- [18] A.T. García-Sosa, M. Oja, C. Hetényi, U. Maran, DrugLogit: Logistic Discrimination between Drugs and Nondrugs Including Disease-Specificity by Assigning Probabilities Based on Molecular Properties. *J. Chem. Inf. Model.* 52 (2012) 2165–2180.
- [19] A.T. García-Sosa, Hydration Properties of Ligands and Drugs in Protein Binding Sites: Tightly-Bound, Bridging Water Molecules and Their Effects and Consequences on Molecular Design Strategies. *J. Chem. Inf. Model.* 53 (2013) 1388–1405.
- [20] A.T. García-Sosa, U. Maran, Drugs, Non-Drugs, and Disease Category Specificity: Organ Effects by Ligand Pharmacology 1. *SAR QSAR Environ. Res.* 24 (2013) 319–331.
- [21] H.-T. Xu, Y. Quan, S.M. Schader, M. Oliveira, T. Bar-Magen, M.A. Wainberg, The M230L Nonnucleoside Reverse Transcriptase Inhibitor Resistance Mutation in HIV-1 Reverse Transcriptase Impairs Enzymatic Function and Viral Replicative Capacity. *Antimicrob. Agents Chemother.* 54 (2010) 2401–2408
- [22] V. Famiglioni, G. La Regina, A. Coluccia, S. Pelliccia, A. Brancale, G. Maga, E. Crespan, R. Badia, E. Riveira-Muñoz, J. A. Esté, R. Ferretti, R. Cirilli, C. Zamperini, M. Botta, D. Schols, V. Limongelli, B. Agostino, E. Novellino, R. Silvestri, Indolylarylsulfones Carrying a Heterocyclic Tail as Very Potent and Broad Spectrum HIV-1 Non-nucleoside Reverse Transcriptase Inhibitors. *J. Med. Chem.* 57 (2014) 9945–9957.
- [23] L. Zhang, X. Tang, Y. Cao, S. Wu, Y. Zhang, J. Zhao, Y. Guo, C. Tian, Z. Zhang, J. Liu, X. Wang, Synthesis and Biological Evaluation of Novel 2-Arylalkylthio-5-iodine-6-substituted-benzyl-pyrimidine-4(3*H*)-ones as Potent HIV-1 Non-Nucleoside Reverse Transcriptase Inhibitors. *Molecules* 19 (2014) 7104-7121.
- [24] X. Chen, P. Zhan, C. Pannecouque, J. Balzarini, E. De Clercq, X. Liu, Synthesis and biological evaluation of piperidine-substituted triazine derivatives as HIV-1 non-nucleoside reverse transcriptase inhibitors. *Eur J Med Chem.* 51 (2012) 60-66.
- [25] R. Menicagli, S. Samaritani, G. Signore, F. Vaglini, L. Dalla Via, In Vitro Cytotoxic Activities of 2-Alkyl-4,6-Diheteroalkyl-1,3,5-Triazines: New Molecules in Anticancer Research. *J. Med. Chem.* 47 (2004) 4649–4652.

- [26] B.R. Henke, T.G. Consler, N. Go, R.L. Hale, D.R. Hohman, S.A. Jones, A.T. Lu, L.B. Moore, J.T. Moore, L.A. Orband-Miller, R.G. Robinett, J. Shearin, P.K. Spearing, E.L. Stewart, P.S. Turnbull, S.L. Weaver, S.P. Williams, G.B. Wisely, M.H. Lambert, A New Series of Estrogen Receptor Modulators That Display Selectivity for Estrogen Receptor Beta. *J. Med. Chem.* 45 (2002) 5492–5505.
- [27] V.K. Pandey, S. Tusi, Z. Tusi, M. Joshi, S. Bajpai, Synthesis and Biological Activity of Substituted 2,4,6-S-Triazines. *Acta Pharm.* 54 (2004) 1–12.
- [28] K. Srinivas, U. Srinivas, V.J. Rao, K. Bhanuprakash, K.H. Kishore, U.S.N. Murty, Synthesis and Antibacterial Activity of 2,4,6-Tri Substituted S-Triazines. *Bioorg. Med. Chem. Lett.* 15 (2005) 1121–1123.
- [29] T. Lübbers, P. Angehrn, H. Gmünder, S. Herzig, J. Kulhanek, Design, Synthesis, and Structure-Activity Relationship Studies of ATP Analogues as DNA Gyrase Inhibitors. *Bioorg. Med. Chem. Lett.* 10 (2000) 821–826.
- [30] A. Ghaib, S. Ménager, P. Vérité, O. Lafont, Synthesis of Various 9,9-Dialkylated Octahydropyrimido [3,4-A]-S-Triazines with Potential Antifungal Activity. *Farmaco* 57 (2002) 109–116.
- [31] S. Lebreton, N. Newcombe, M. Bradley, Antibacterial Single-Bead Screening. *Tetrahedron* 59 (2003) 10213–10222.
- [32] G.A. McKay, R. Reddy, F. Arhin, A. Belley, D. Lehoux, G. Moeck, I. Sarmiento, T.R. Parr, P. Gros, J. Pelletier, A.R. Far, Triaminotriazine DNA Helicase Inhibitors with Antibacterial Activity. *Bioorg. Med. Chem. Lett.* 16 (2006) 1286–1290.
- [33] Z.E. Koc, H. Bingol, A.O. Saf, E. Torlak, A. Coskun, Synthesis of Novel Tripodal-Benzimidazole from 2,4,6-Tris(p-Formylphenoxy)-1,3,5-Triazine: Structural, Electrochemical and Antimicrobial Studies. *J. Hazard. Mater.* 183 (2010) 251–255.
- [34] A. Kumar, S.K. Menon, Fullerene Derivatized S-Triazine Analogues as Antimicrobial Agents. *Eur. J. Med. Chem.* 44 (2009) 2178–2183.
- [35] C.-F. Chang, C.-Y. Huang, Y.-C. Huang, K.-Y. Lin, Y.-J. Lee, C.-J. Wang, Total Synthesis of (±)-Armapavines and (±)-Nuciferines From (2-Nitroethyl)benzene Derivatives. *Synth. Commun.* 40 (2010) 3452–3466.
- [36] C.A.M. Afonso, N.M.T. Lourenço, A. de A. Rosatella, Synthesis of 2,4,6-Tri-Substituted-1,3,5-Triazines. *Molecules* 11 (2006) 81–102.
- [37] Y.-Z. Xiong, F.-E. Chen, J. Balzarini, E. De Clercq, C. Pannecouque, Non-Nucleoside HIV-1 Reverse Transcriptase Inhibitors. Part 11: Structural Modulations of Diaryltriazines with Potent Anti-HIV Activity. *Eur. J. Med. Chem.* 43 (2008) 1230–1236.
- [38] J. Xie, C. Xu, N. Kohler, Y. Hou, S. Sun, Controlled PEGylation of Monodisperse Fe<sub>3</sub>O<sub>4</sub> Nanoparticles for Reduced Non-Specific Uptake by Macrophage Cells. *Adv. Mater.* 19 (2007) 3163–3166.
- [39] Z.E. Koç, Ş. Uysal, Synthesis and Characterization of Tripodal Oxy-Schiff Base (2,4,6-Tris(4-Carboxymethylenephylimino-4'-Formylphenoxy)-1,3,5-Triazine) and the

- Thermal and Magnetic Properties of Its Fe(III)/Cr(III) Complexes. *J. Inorg. Organomet. Polym. Mater.* 21 (2011) 400–406.
- [40] M. Venkatraj, K.K. Ariën, J. Heeres, J. Joossens, B. Dirié, S. Lyssens, J. Michiels, P. Cos, P.J. Lewi, G. Vanham, L. Maes, P. Van der Veken, K. Augustyns, From Human Immunodeficiency Virus Non-Nucleoside Reverse Transcriptase Inhibitors to Potent and Selective Antitrypanosomal Compounds. *Bioorg. Med. Chem.* 22 (2014) 5241–5248.
- [41] Protein Data Bank. Research Collaboratory for Structural Bioinformatics <http://www.rcsb.org/pdb/home/home.do> (accessed Apr 7, 2010)
- [42] D.W. Ludovici, R.W. Kavash, M.J. Kukla, C.Y. Ho, H. Ye, B.L. De Corte, K. Andries, M.P. de Béthune, H. Azijn, R. Pauwels, H.E. Moereels, J. Heeres, L.M. Koymans, M.R. de Jonge, K.J. Van Aken, F.F. Daeyaert, P.J. Lewi, K. Das, E. Arnold, P.A. Janssen, Evolution of Anti-HIV Drug Candidates. Part 2: Diaryltriazine (DATA) Analogues. *Bioorg. Med. Chem. Lett.* 11 (2001) 2229–2234.
- [43] K. Das, P.J. Lewi, S.H. Hughes, E. Arnold, Crystallography and the Design of Anti-AIDS Drugs: Conformational Flexibility and Positional Adaptability Are Important in the Design of Non-Nucleoside HIV-1 Reverse Transcriptase Inhibitors. *Prog. Biophys. Mol. Biol.* 88 (2005) 209–231.
- [44] K. Das, A.D. Clark, P.J. Lewi, J. Heeres, M.R. de Jonge, L.M.H. Koymans, H.M. Vinkers, F. Daeyaert, D.W. Ludovici, M.J. Kukla, B. De Corte, R.W. Kavash, C.Y. Ho, H. Ye, M.A. Lichtenstein, K. Andries, R. Pauwels, M.-P. de Béthune, P.L. Boyer, P. Clark, S.H. Hughes, P.A.J. Janssen, E. Arnold, Roles of Conformational and Positional Adaptability in Structure-Based Design of TMC125-R165335 (Etravirine) and Related Non-Nucleoside Reverse Transcriptase Inhibitors That Are Highly Potent and Effective against Wild-Type and Drug-Resistant HIV-1 Variants. *J. Med. Chem.* 47 (2004) 2550–2560.
- [45] R. Pauwels, New Non-Nucleoside Reverse Transcriptase Inhibitors (NNRTIs) in Development for the Treatment of HIV Infections. *Curr. Opin. Pharmacol.* 4 (2004) 437–446.
- [46] J. Hladikova, H.E. Fischer, P. Jungwirth, P.E. Mason, Hydration of Hydroxyl And Amino Groups Examined By Molecular Dynamics And Neutron Scattering. *J. Phys Chem. B* 119 (2015), 6357–6365.
- [47] Glide, version 5.9; Schrödinger, LLC; New York, 2013.
- [48] B. Pogorelčnik, M. Brvar, I. Zajc, M. Filipič, T. Solmajer, A. Perdih, Monocyclic 4-amino-6-(phenylamino)-1,3,5-triazines as Inhibitors of Human DNA Topoisomerase I $\alpha$ . *Bioorg. Med. Chem. Lett.* 14 (2014) 5762–5768.
- [49] B. Pogorelčnik, M. Janežič, I. Sosič, S. Gobec, T Solmajer, A. Perdih, 4,6-Substituted-1,3,5-triazin-2(1H)-ones as Monocyclic Catalytic Inhibitors of Human DNA Topoisomerase I $\alpha$  Targeting the ATP Binding Site, *Bioorg. Med. Chem.* 23 (2015) 4218–4229.
- [50] J.A. Wells, C.L. McClendon, Reaching for High-Hanging Fruit in Drug Discovery at Protein-Protein Interfaces. *Nature* 459 (2007) 1001–1009.



- [51] MacroModel, version 9.9; Schrödinger, LLC; New York, 2012.
- [52] Protein Preparation Wizard, version 1.0; Schrödinger, LLC; New York, 2009.
- [53] T. Cheng, Y. Zhao, X. Li, F. Lin, Y. Xu, X. Zhang, Y. Li, R. Wang, L. Lai, Computation of Octanol-Water Partition Coefficients by Guiding an Additive Model with Knowledge. *J. Chem. Inf. Model.* 47 (2007) 2140–2148.
- [54] S. Vahur, A. Teearu, T. Haljasorg, P. Burk, I. Leito, I. Kaljurand, Analysis of dammar resin with MALDI-FT-ICR-MS and APCI-FT-ICR-MS. *J. Mass Spectrom.* 47 (2012) 392–409.
- [55] I. Kaljurand, T. Rodima, A. Pihl, V. Mäemets, I. Leito, I. A. Koppel, M. Mishima, Acid–Base Equilibria in Nonpolar Media. 4. Extension of the Self-Consistent Basicity Scale in THF Medium. Gas-Phase Basicities of Phosphazenes. *J. Org. Chem.* 68 (2003) 9988–9993.
- [56] A.A. Kolomeitsev, I. A. Koppel, T. Rodima, J. Barten, E. Lork, G.-V. Rösenthaller, I. Leito, Guanidinophosphazenes: Design, Synthesis, and Basicity in THF and in the Gas Phase. *J. Am. Chem. Soc.* 127 (2005) 17656–17666.
- [57] K.A. Clouse, D. Powell, I. Washington, G. Poli, K. Strebel, W. Farrar, P. Barstad, J. Kovacs, A.S. Fauci, T.M. Folks, Monokine Regulation of Human Immunodeficiency Virus-1 Expression in a Chronically Infected Human T Cell Clone. *J. Immunol.* 142 (1989) 431–438.
- [58] E.J. Duh, W.J. Maury, T.M. Folks, A.S. Fauci, A.B. Rabson, Tumor Necrosis Factor Alpha Activates Human Immunodeficiency Virus Type 1 through Induction of Nuclear Factor Binding to the NF-Kappa B Sites in the Long Terminal Repeat. *Proc. Natl. Acad. Sci. U. S. A.* 86 (1989) 5974–5978.
- [59] E.J. Platt, M. Bilaska, S.L. Kozak, D. Kabat, D.C. Montefiori, Evidence That Ecotropic Murine Leukemia Virus Contamination in TZM-B1 Cells Does Not Affect the Outcome of Neutralizing Antibody Assays with Human Immunodeficiency Virus Type 1. *J. Virol.* 83 (2009) 8289–8292.
- [60] Y. Takeuchi, M.O. McClure, M. Pizzato, Identification of Gammaretroviruses Constitutively Released from Cell Lines Used for Human Immunodeficiency Virus Research. *J. Virol.* 82 (2008) 12585–12588.
- [61] X. Wei, J.M. Decker, H. Liu, Z. Zhang, R.B. Arani, J.M. Kilby, M.S. Saag, X. Wu, G.M. Shaw, J.C. Kappes, Emergence of Resistant Human Immunodeficiency Virus Type 1 in Patients Receiving Fusion Inhibitor (T-20) Monotherapy. *Antimicrob. Agents Chemother.* 46 (2002) 1896–1905.
- [62] C.A. Derdeyn, J.M. Decker, J.N. Sfakianos, X. Wu, W.A. O'Brien, L. Ratner, J.C. Kappes, G.M. Shaw, E. Hunter, Sensitivity of Human Immunodeficiency Virus Type 1 to the Fusion Inhibitor T-20 Is Modulated by Coreceptor Specificity Defined by the V3 Loop of gp120. *J. Virol.* 74 (2000) 8358–8367.

- [63] E.J. Platt, K. Wehrly, S.E. Kuhmann, B. Chesebro, D. Kabat, Effects of CCR5 and CD4 Cell Surface Concentrations on Infections by Macrophagetropic Isolates of Human Immunodeficiency Virus Type 1. *J. Virol.* 72 (1998) 2855–2864.
- [64] D. D. Richman, D. Havlir, J. Corbeil, D. Looney, C. Ignacio, S. A. Spector, J. Sullivan, S. Cheeseman, K. Barringer, D. Pauletti, Nevirapine resistance mutations of human immunodeficiency virus type 1 selected during therapy. *J. Virol.* 68, (1194) 1660–6.
- [65] J.C. Kappes, X. Wu, (2004). U.S. Patent No. 6,797,462. Birmingham, AL: U.S.

ACCEPTED MANUSCRIPT

